*Article*

# Association between Left Atrial Function and Survival in Systemic Sclerosis

Adrian Giucă [1,2,3,†], Xavier Galloo [1,4,†], Maria Chiara Meucci [1,5,†], Steele C. Butcher [1,6,†], Bogdan Alexandru Popescu [2,7,†], Ruxandra Jurcuț [2,7,†], Adrian Săftoiu [7,8,†], Ciprian Jurcuț [9,†], Laura Groșeanu [7,10,†], Anca Emanuela Mușetescu [11,†], Saad Ahmed [12,†], Jeska De Vries-Bouwstra [12,†], Jeroen J. Bax [1,†] and Nina Ajmone Marsan [1,*,†]

1 Department of Cardiology, Heart Lung Center, Leiden University Medical Center, Albinusdreef 2, 2300 RC Leiden, The Netherlands; adriangiuca17@gmail.com (A.G.); x.galloo@lumc.nl (X.G.); mariachiarameucci@gmail.com (M.C.M.); s.c.butcher@lumc.nl (S.C.B.); j.j.bax@lumc.nl (J.J.B.)
2 "Prof. Dr. C.C. Iliescu" Emergency Institute for Cardiovascular Diseases, Fundeni Street 258, 022328 Bucharest, Romania; bogdan.a.popescu@gmail.com (B.A.P.); rjurcut@gmail.com (R.J.)
3 Department of Internal Medicine, Craiova University of Medicine and Pharmacy, Petru Rares 2, 200349 Craiova, Romania
4 Department of Cardiology, Vrije Universiteit Brussel (VUB), Universitair Ziekenhuis Brussel (UZ Brussel), Avenue du Laerbeek 101, 1090 Jette, Brussels, Belgium
5 Department of Cardiovascular Medicine, Fondazione Policlinico Universitario A. Gemelli IRCCS, Via Giuseppe Moscati 31, 00168 Rome, Italy
6 Department of Cardiology, Royal Perth Hospital, Perth, Western Australia, 197 Wellington Street, Perth, WA 6000, Australia
7 Faculty of Medicine, "Carol Davila" University of Medicine and Pharmacy, Eroii Sanitari Bvd no. 8, 050474 Bucharest, Romania; adriansaftoiu@gmail.com (A.S.); laura.groseanu@gmail.com (L.G.)
8 Department of Gastroenterology and Hepatology, Elias University Emergency Hospital, Marasti Bvd 17, 011461 Bucharest, Romania
9 Department of Internal Medicine, "Carol Davila" Central Military Emergency University Hospital, Calea Plevnei 134, 010825 Bucharest, Romania; cjurcut@gmail.com
10 Department of Rheumatology, "Sf. Maria" Clinical Hospital, Ion Mihalache Bvd 37–39, 011172 Bucharest, Romania
11 Department of Rheumatology, Craiova University of Medicine and Pharmacy, Petru Rares 2, 200349 Craiova, Romania; anca.musetescu@umfcv.ro
12 Department of Rheumatology, Leiden University Medical Center, 2333 ZA Leiden, The Netherlands; s.ahmed@lumc.nl (S.A.); j.k.de_vries-bouwstra@lumc.nl (J.D.V.-B.)
* Correspondence: n.ajmone@lumc.nl; Tel.: +31-71-526-2020; Fax: +31-71-526-6809
† These authors contributed equally to this work.

**Abstract:** Systemic sclerosis (SSc) is a multisystemic autoimmune disorder in which cardiac involvement is frequent and portends negative prognosis. Left ventricular (LV) diastolic dysfunction is one of the most common cardiac alterations in these patients, and left atrial (LA) reservoir strain ($\varepsilon_R$) measurement using speckle tracking echocardiography has been proposed as a novel parameter for a better assessment of LV diastolic function. Therefore, the aim of this study was to test the prognostic value of $\varepsilon_R$ in a large multicenter cohort of SSc patients. In total, 311 SSc patients (54 ± 14 years, 85% female) were included from two different centers. Echocardiography was performed at the time of first visit, including $\varepsilon_R$ measurement. Over a median follow-up of 132 (interquartile range: 110 to 157) months, 67 (21.5%) patients experienced the outcome of all-cause mortality. Spline curve analysis identified an optimal cut-off value of 30% for $\varepsilon_R$, and patients with $\varepsilon_R \leq 30\%$ showed a 10-year cumulative survival rate of 71% as compared to 88% for patients with $\varepsilon_R > 30\%$ (log-rank $p < 0.001$). At the multivariable Cox regression analysis, $\varepsilon_R$ was independently associated with the endpoint (HR 1.830; 95% confidence interval (CI) 1.031–3.246; $p = 0.039$) together with age (HR 1.071, 95% CI 1.043 to 1.099; $p < 0.001$), sex (female) (HR 0.444, 95% CI 0.229 to 0.861; $p = 0.016$), and diffusing lung capacity for carbon monoxide (HR 0.969 95% CI 0.956 to 0.982; $p < 0.001$). $\varepsilon_R$ is of independent prognostic value in SSc and might help optimizing risk stratification in these patients.

## 1. Introduction

Systemic sclerosis (SSc) is a rare chronic autoimmune disorder, with multi-organ involvement and relatively frequent cardiac abnormalities, including left ventricle (LV) systolic and diastolic dysfunction, myocardial fibrosis, as well as conduction and rhythm disturbances, which are associated with adverse clinical outcomes [1].

Particularly, LV diastolic dysfunction has been shown to be an important prognosticator in patients with SSc, but its accurate assessment remains challenging [2]. Current recommendations propose an echocardiographic multi-parametric algorithm, in which maximum left atrium (LA) volume index (LAVi) plays an important role, together with pulmonary pressure estimation, mitral inflow and Tissue Doppler parameters [3]. However, compared to the gold standard of right heart catheterization, this approach still has limited diagnostic accuracy to determine elevated LV filling pressures, and LA strain measurement by speckle tracking echocardiography (STE) has been proposed to improve it. Particularly, LA strain measured during the reservoir phase ($\varepsilon_R$), reflecting mainly atrial compliance and therefore possibly also atrial fibrosis, has been more recently added to the diagnostic algorithm of LV diastolic dysfunction and was shown to be impaired in different patient populations, preceding LA remodeling and dilation [4–6].

Initial studies in SSc patients have shown $\varepsilon_R$ to be reduced compared to controls even before changes in conventional systolic/diastolic function parameters occurred. Also, studies measuring LA strain with cardiac magnetic resonance imaging suggested a potential prognostic value of this measurement in SSc [7–9]. We therefore sought to identify if $\varepsilon_R$ impairment assessed by echocardiography was associated with all-cause mortality in a large multi-center cohort of SSc patients.

## 2. Materials and Methods

### 2.1. Patient Population

From 2003 until 2019, SSc patients referred for a specifically designed multidisciplinary healthcare program at the Department of Rheumatology of the Leiden University Medical Centre (The Netherlands), and at "Prof. Dr. C. C. Iliescu" Emergency Institute for Cardiovascular Diseases (Bucharest, Romania), and who had a complete comprehensive two-dimensional transthoracic echocardiogram (2DTTE) were included [10]. SSc cases were diagnosed according to the classification system proposed by LeRoy and Medsger [11]. Baseline 2DTTE was selected according to the date of the first visit in the care program of both centers. Exclusion criteria were the following: (1) history of myocardial infarction or severe valvular heart disease; (2) image quality and acquisition not sufficient for LA assessment. Written informed consent was obtained at the time of inclusion in the multidisciplinary healthcare program as was approved by the institutional ethical committee (REU 043). This specific retrospective analysis was approved by the institutional review board of both centers.

### 2.2. Clinical Variables

Disease-related characteristics such as SSc subtype (diffuse or limited), modified Rodnan Skin Score (mRSS), Raynaud's phenomenon, proximal muscle weakness, synovitis, digital ulcerations, and pitting scars were reported. General medical history, medication use, and cardiovascular risk factors were also noted. Laboratory tests were comprised from N-terminal pro-B natriuretic peptide (NTproBNP), creatine kinase and renal function (assessed by the estimated glomerular filtration rate (eGFR) by the Modification of Diet in Renal Disease formula).

Pulmonary function was assessed by spirometry, including percentage of predicted values for forced vital capacity (FVC), forced expiratory volume in 1 s (FEV1) and dif-

fusing lung capacity for carbon monoxide (DLCO). Presence of pulmonary fibrosis was investigated by high-resolution computed tomography [12,13].

### 2.3. Standard 2DTTE

All patients underwent echocardiography in the left lateral decubitus position using available ultrasound system (Vivid 7, E9 and E95; GE—Vingmed, Milwaukee, Wisconsin) and 3.5—MHz or 5—MHz transducers. Standard M-mode and 2-dimensional, color, pulsed, and continuous wave Doppler images were acquired. A commercially available software—EchoPAC (version 113; GE—Vingmed) was used to digitally store all images for off-line analysis. Images were then analyzed with the dedicated software by an expert reader (AG) with no clinical relationship with the patients.

LV end-diastolic diameter (LVEDD), end-systolic volume (LVESV), ejection fraction (LVEF) and LAVi were measured according to the current guidelines [14]. LV diastolic function was further assessed using multiple parameters: peak early (E) and late (A) diastolic velocities and E-wave deceleration time (DTE), measured on pulsed-wave Doppler recordings of the transmitral flow; E/A ratio; e prime (e') measured with tissue Doppler imaging (TDI) at the septal and lateral side of the mitral annulus in the apical 4-chamber view; average E/e' ratio was then calculated [3]. When possible, pulmonary artery systolic pressure (PASP) was estimated by determining the right ventricular (RV) systolic pressure, calculated from the peak gradient of the tricuspid regurgitation, to which the value of the right atrial pressure estimated by inferior vena cava dimensions and respiratory collapse was added. RV systolic function was assessed by measuring the tricuspid annular plane systolic excursion (TAPSE) on M-mode echocardiography [15]. Pericardial effusion was also noted.

### 2.4. Two-Dimensional STE

LV strain was measured in the longitudinal direction, using the 3 standard apical views: 4-chamber, 2-chamber, and 3-chamber. LV global longitudinal strain (GLS) was automatically calculated as the average peak systolic strain of 17 LV segments and expressed as absolute values: the higher the value, the better the myocardial shortening [14].

For measuring LA longitudinal strain, a dedicated non-foreshortened apical 4-chamber view was used, and the endocardial border tracing was started at the septal part of the mitral annulus, extrapolated across the pulmonary veins and LA appendage and ended at the opposite mitral annulus side (Figure 1) [16].

From the LA strain curve, $\varepsilon_R$ was measured as the positive peak systolic value within LV end-diastole (mitral valve closure) and mitral valve opening [16]. The zero-reference point was chosen at LV end-diastole (onset of QRS). $\varepsilon_R$ was selected as the parameter to assess LA function, since it was shown in previous literature to have the best reproducibility and feasibility (also in atrial fibrillation patients) and the strongest prognostic value [17–19].

### 2.5. Study Endpoint

An endpoint of all-cause mortality was used. All-cause mortality data were obtained by retrieval of survival status through the municipal civil registries. Time until death was calculated from the initial 2DTTE till date of event.

### 2.6. Statistical Analysis

Categorical variables are expressed as absolute frequencies and percentages. Continuous variables are presented as mean $\pm$ SD in case of normal distribution, and as median (interquartile range—IQR) in cases of non-normal distribution. Adherence to normality was assessed by normality tests. Comparison between the groups was performed using the Pearson $\chi^2$ test for categorical variables and the Mann–Whitney U-test for continuous variables with normal distribution, and Kruskal–Wallis for non-normally distributed continuous variables.
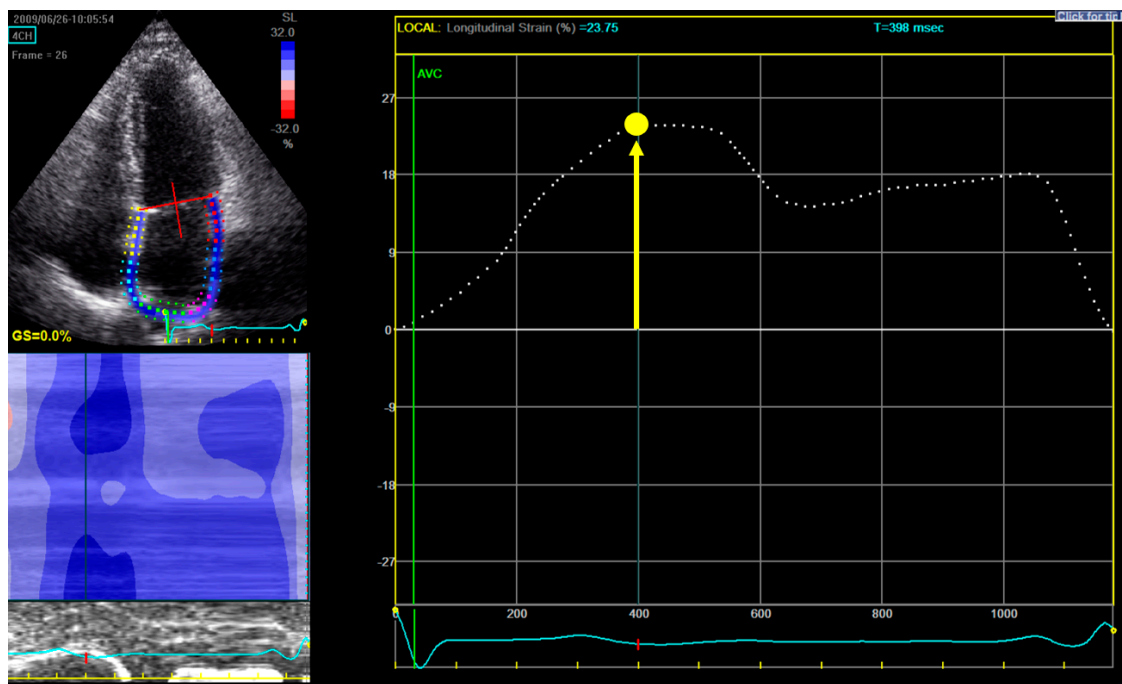
**Figure 1.** Measurement of left atrial reservoir strain ($\varepsilon_R$). Upper-left panel shows the selection of the region of interest: in a dedicated non-foreshortened apical 4 chamber view, the tracing begins at the level of the endocardial border of the mitral annulus; it is then continued along the endocardial surface of the left atrium extrapolating across the orifices of the pulmonary veins and left atrial appendage, ending at the opposite side of the mitral annulus. Right panel displays the left atrium longitudinal strain curve: the zero-reference point is at end-diastole and $\varepsilon_R$ is calculated as the difference between the strain value at the mitral valve opening and ventricular end-diastole (positive value). In this example in a patient from our study, $\varepsilon_R$ is 23.75%.

Penalized spline curve analysis was fitted, demonstrating a continuous increase in HR for all-cause mortality across a range of $\varepsilon_R$ values. To dichotomize the study population for Kaplan–Meier analysis, a cut-off value of 30% was estimated to be the ideal value (i.e., where the predicted HR for all-cause mortality was $\geq 1$).

Kaplan–Meier curves were used to estimate the 10-year survival rates, and differences between the 2 groups (i.e., by using the $\varepsilon_R$ cut-off) were tested with the Mantel-Cox log-rank test.

To investigate the association between clinical and echocardiographic parameters with the occurrence of the endpoint, univariable Cox Regression was performed. Variables with a univariable value of $p < 0.05$ were incorporated into a multivariable model but avoiding collinearity among different variables and overfitting the model based on the number of events. The hazard ratio (HR) and 95% confidence intervals (CI) were reported for each variable. All tests were two-sided and $p$ values $< 0.05$ were considered to be statistically significant. Data analysis was performed using SPSS for Windows, version 25 (IBM Corp., Armonk, New York, NY, USA) and R version 4.0.1 (R Foundation for Statistical Computing, Vienna, Austria).

## 3. Results

### 3.1. Study Population: Clinical and Echocardiographic Characteristics

In total, 375 patients were selected, but 64 patients were further excluded because of insufficient image quality for LA analysis. Therefore, the final analysis included 311 SSc cases, whose clinical and echocardiographic characteristics are summarized in Table 1.

**Table 1.** Clinical and echocardiographic characteristics of the study population and comparison between cases with $\varepsilon_R \leq 30\%$ and $\varepsilon_R > 30\%$. Values are presented as mean $\pm$ SD, median (IQR) or n (%). ACEi—angiotensin-converting enzyme inhibitors; ARB—angiotensin receptor blockers; AZA—azathioprine; CSs—corticosteroids; CYC—cyclophosphamide; dcSSc—diffuse cutaneous SSc; DLCO—diffusing lung capacity for carbon monoxide; eGFR—estimated glomerular filtration rate; FEV1—forced expiratory volume in 1 s; FVC—forced vital capacity; LAVi—left atrial volume index; lcSSc—limited cutaneous SSc; LVEDD—left ventricular end-diastolic diameter; LVEF—left ventricle ejection fraction; LVESV—left ventricular end-systolic volume; LV GLS—left ventricle global longitudinal strain; mRSS—modified Rodnan Skin Score; MTX—methotrexate; NTproBNP—N-terminal fragment of the pro-B natriuretic peptide; PASP—pulmonary artery systolic pressure; RV—right ventricle; SSc—systemic sclerosis; TAPSE—tricuspid annular plane systolic excursion; $\varepsilon_R$—left atrial reservoir strain.

| Variable | Overall Population (n = 311) | $\varepsilon_R \leq 30\%$ (n = 106) | $\varepsilon_R > 30\%$ (n = 205) | *p*-Value |
|---|---|---|---|---|
| Age (years) | 53 ($\pm$14) | 61 ($\pm$12) | 50 ($\pm$14) | *<0.001* |
| Sex (female) | 264 (85%) | 88 (83%) | 176 (86%) | 0.508 |
| SSc subtype | 174 (70%) lcSSc / 76 (30%) dcSSc | 62 (70%) lcSSc / 26 (30%) dcSSc | 112 (69%) lcSSc / 50 (31%) dcSSc | 0.829 |
| Time from first non-Raynaud's phenomenon symptom to diagnosis (years) | 3 (0–17) | 0.5 (−5–20) | 3 (0–12) | 0.820 |
| Time from onset of Raynaud's phenomenon to diagnosis (years) | 2 (0–10) | 2 (0–14) | 2 (0–9) | 0.948 |
| mRSS | 4 (1–6) | 4 (2–7) | 3 (0–6) | 0.118 |
| Raynaud's phenomenon | 301 (97%) | 100 (94%) | 201 (98%) | 0.067 |
| Digital ulcerations | 68 (22%) | 18 (17%) | 50 (24%) | 0.129 |
| Pitting scars | 125 (40%) | 37 (35%) | 88 (43%) | 0.161 |
| Proximal muscle weakness | 27 (9%) | 12 (11%) | 15 (7.5%) | 0.256 |
| Synovitis | 35 (12%) | 11 (10.5%) | 24 (12%) | 0.659 |
| Atrial fibrillation | 15 (5%) | 10 (9.4%) | 5 (2.4%) | *0.006* |
| Hypertension | 89 (29%) | 45 (42.5%) | 44 (21%) | *<0.001* |
| Smoking | 148 (48%) | 58 (55%) | 90 (44%) | 0.076 |
| Diabetes mellitus | 13 (4%) | 4 (3.8%) | 9 (4.4%) | 1 |
| Coronary artery disease | 13 (4%) | 6 (5.7%) | 7 (3.4%) | 0.353 |
| NTproBNP (pg/mL) | 93.8 (53.9–191) | 127 (57.6–291) | 85 (53–152) | *0.001* |
| Creatine kinase (U/L) | 85 (60–120.7) | 84 (58–140) | 85 (61–117) | 0.982 |
| eGFR (ml/min/1.73 m$^2$) | 89.4 ($\pm$26) | 89 ($\pm$26) | 92 ($\pm$26) | *0.009* |
| DLCO (%pred) | 64.2 ($\pm$19) | 60 ($\pm$18) | 66 ($\pm$19) | *0.012* |
| FEV1 (%pred) | 95 ($\pm$19.3) | 93 ($\pm$19.2) | 96 ($\pm$19.4) | 0.291 |
| FVC (%pred) | 101 ($\pm$22) | 99 ($\pm$22.6) | 102.3 ($\pm$22) | 0.317 |
| LVEDD (mm) | 47.2 ($\pm$5.4) | 47.5 ($\pm$5.7) | 47 ($\pm$5) | 0.429 |
| LVESV (ml) | 30 (24–39) | 31 (25–40) | 30 (24–39) | 0.258 |
| LVEF (%) | 62 ($\pm$6.5) | 60.3 ($\pm$7.3) | 62.6 ($\pm$5.8) | *0.003* |
| LV GLS (%) | 21 (19.5–22) | 20.4 (18–21.6) | 21 (20–22) | *<0.001* |
| LAVi (ml/m$^2$) | 21.8 (17.3–29) | 24.2 (19.8–30.8) | 20.7 (16–27.3) | *<0.001* |
| $\varepsilon_R$ (%) | 35.7 ($\pm$11.4) | 23.9 ($\pm$4.2) | 41.7 ($\pm$9) | *<0.001* |
| E wave (cm/sec) | 78.2 ($\pm$18.3) | 77 ($\pm$22) | 78.6 ($\pm$16) | 0.554 |
| A wave (cm/sec) | 71 (58–89) | 75 (64–96) | 69 (57–83) | *0.009* |
| E/A ratio | 1.04 (0.8–1.3) | 0.95 (0.77–1.1) | 1.1 (0.89–1.3) | *<0.001* |
| E/e' ratio | 8.5 (7–10.7) | 10 (8–12) | 8 (7–10) | *<0.001* |
| TAPSE (mm) | 22.6 ($\pm$3.7) | 22 ($\pm$4) | 23 ($\pm$3) | *0.013* |
| Moderate or severe tricuspid regurgitation | 18 (17%) | 11 (23%) | 7 (12%) | 0.150 |
| Tricuspid regurgitation maximum gradient (mmHg) | 22 (18–27) | 24 (18–29) | 21.5 (18.3–25) | *0.028* |
| PASP (mmHg) | 25 (21.2–30) | 27 (21–30.7) | 24.7 (21.3–28.6) | 0.190 |
| Pericardial effusion | 17 (5.5%) | 8 (7.6%) | 9 (4.4%) | 0.237 |
| Medication | | | | |
| ACEi or ARB | 118 (38%) | 51 (48%) | 67 (33%) | *0.010* |
| Beta-blocker | 27 (8.7%) | 16 (15%) | 11 (5.4%) | 0.060 |
| CSs | 45 (14.5%) | 15 (14.2%) | 30 (14.7%) | 0.520 |
| CYC | 7 (2.3%) | 1 (1%) | 6 (3%) | 0.429 |
| MTX | 42 (13.5%) | 17 (16%) | 25 (12%) | 0.384 |
| AZA | 17 (5.5%) | 6 (5.7%) | 11 (5.4%) | 0.555 |

Median time from first non-Raynaud symptom till diagnosis was 3 (IQR 0–17) years, and from Raynaud symptom till diagnosis 2 (IQR 0–10) years. Most cases (70%) were

diagnosed as having limited cutaneous SSc (lcSSc) and lung fibrosis was present in 45% of patients.

On average, LV function was preserved as assessed by LVEF ($62 \pm 6.5\%$) and LV GLS (median 21%, IQR 19.5–22). LAVi had a median value of 21.8 mL/m$^2$ (IQR 17.3–29), and $\varepsilon_R$ a mean value of 35.7% ($\pm$ 11.4). Pulmonary pressures were in average within normal range (median PASP 25 mmHg, IQR 21–30 mmHg). Few patients exhibited pericardial effusion (5.5%).

### 3.2. Endpoint Analysis

Over a median follow-up of 132 (IQR 110–157) months, a total of 67 patients (21.5%) experienced the endpoint.

Spline curve analysis (Figure 2) showed increase in the HR for all-cause death with progressively lower values of $\varepsilon_R$, and a value of 30% was selected as the optimal cut-off for $\varepsilon_R$.
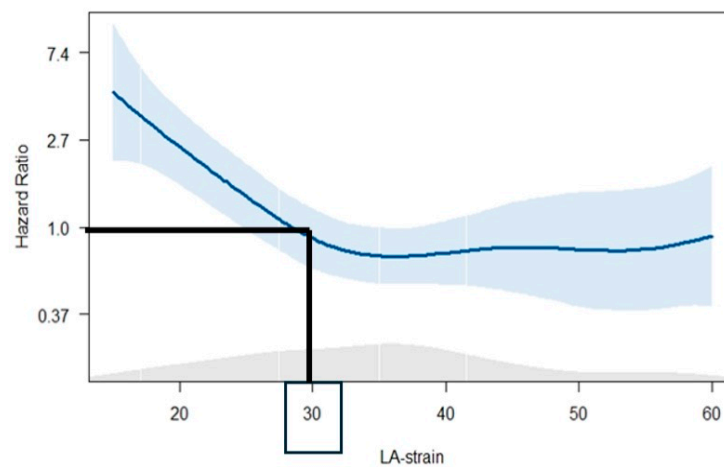


**Figure 2.** Spline curve demonstrating the HR for all-cause mortality across a range of values of $\varepsilon_R$.

Kaplan–Meier analysis demonstrated significantly worse event-free survival for patients with $\varepsilon_R \leq 30\%$, when compared to $\varepsilon_R > 30\%$ (Figure 3). In particular, the 10-year cumulative survival rate was 82% for the total population, with 71% and 88% for patients with $\varepsilon_R \leq 30\%$ and $\varepsilon_R > 30\%$, respectively (log-rank $p < 0.001$).
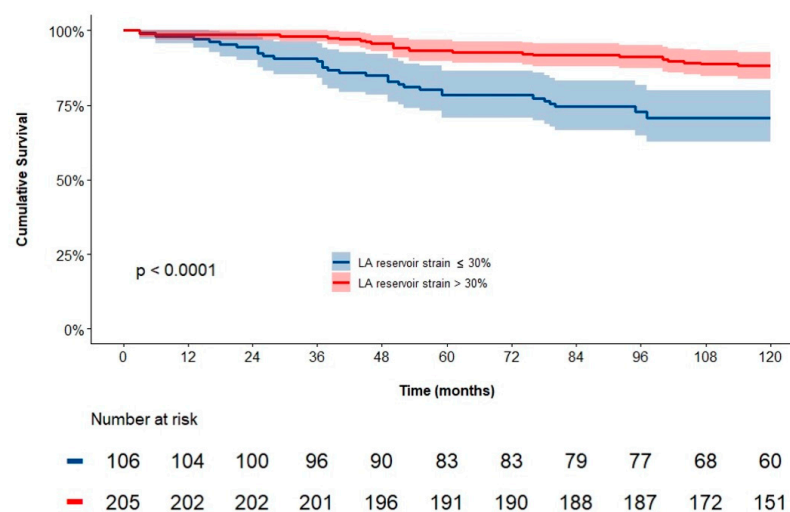


**Figure 3.** Kaplan–Meier curve for the endpoint of all-cause death at 10 years of follow-up for patients divided according to the cut-off value of $\varepsilon_R$ of 30%.

According to the univariate Cox regression analysis (Table 2), the following clinical and echocardiographic variables were associated with all-cause death: age, sex, SSc subtype, mRSS, pulmonary fibrosis, NTproBNP, DLCO, LV GLS, LAVi, $\varepsilon_R \leq 30\%$, E/e', and PASP.

**Table 2.** Univariable Cox regression analysis to identify clinical and echocardiographic variables associated with all-cause mortality. HR—hazard ratio; CI—confidence interval; abbreviations as in Table 1.

| Variable | Univariable Analysis | |
|---|---|---|
| | HR (95% CI) | *p* value |
| Age (years) | 1.060 (1.038–1.082) | *<0.001* |
| Sex (female) | 0.445 (0.259–0.765) | *0.003* |
| SSc subtype | 1.823 (1.099–3.026) | *0.020* |
| mRSS | 1.048 (1.027–1.069) | *<0.001* |
| Pulmonary fibrosis | 2.750 (1.636–4.621) | *<0.001* |
| NTproBNP (pg/mL) | 1.001 (1.001–1.001) | *<0.001* |
| Creatine kinase (U/L) | 1.000 (0.998–1.002) | 0.954 |
| eGFR (mL/min/1.73 m$^2$) | 0.993 (0.985–1.002) | 0.119 |
| DLCO (%pred) | 0.963 (0.953–0.974) | *<0.001* |
| LVEDD (mm) | 1.016 (0.972–1.062) | 0.478 |
| LVESV (mL) | 1.008 (0.991–1.025) | 0.383 |
| LVEF (%) | 0.975 (0.942–1.010) | 0.164 |
| LV GLS (%) | 0.771 (0.716–0.830) | *<0.001* |
| LAVi (mL/m$^2$) | 1.041 (1.018–1.065) | *<0.001* |
| $\varepsilon_R$ ($\leq 30\%$) | 2.460 (1.522–3.975) | *<0.001* |
| E wave (cm/s) | 0.999 (0.985–1.013) | 0.884 |
| E/e' ratio | 1.070 (1.023–1.119) | *0.003* |
| TAPSE (mm) | 0.960 (0.900–1.023) | 0.209 |
| PASP (mmHg) | 1.086 (1.061–1.112) | *<0.001* |
| Pericardial effusion | 0.805 (0.253–2.564) | 0.714 |
| Hypertension | 1.927 (1.178–3.154) | *0.009* |
| Atrial fibrillation | 2.098 (0.906–4.856) | 0.084 |

On multivariate Cox regression analysis, $\varepsilon_R \leq 30\%$ was independently associated with the endpoint (HR 1.830, 95% CI 1.031 to 3.246; $p = 0.039$) together with age (HR 1.071, 95% CI 1.043 to 1.099; $p < 0.001$), sex (female) (HR 0.444, 95% CI 0.229 to 0.861; $p = 0.016$), and DLCO (HR 0.969 95% CI 0.956 to 0.982; $p < 0.001$); other variables did not reach statistical significance.

### 3.3. Difference in Clinical and Echocardiographic Variables According to $\varepsilon_R$

To further characterize the patients according to $\varepsilon_R$ values, clinical and echocardiographic characteristics were compared between patients with $\varepsilon_R \leq 30\%$ and >30% (Table 1). In total, 106 (34%) SSc cases presented $\varepsilon_R$ values $\leq 30\%$. Patients in this group were older, had a higher prevalence of systemic hypertension and atrial fibrillation, but did not show significant difference in terms of SSc-related characteristics. However, they showed more impaired pulmonary function (namely reduced DLCO) and kidney function and higher values of NTproBNP. By echocardiography, patients with $\varepsilon_R \leq 30\%$ were also characterized by lower LVEF, lower LV GLS, and larger LAVi; they also showed higher values of E/e' and lower TAPSE.

## 4. Discussion

The main findings of the current study can be summarized as follows: (1) in a large multicenter cohort, SSc patients with impaired left atrium function, defined as $\varepsilon_R \leq 30\%$ showed lower survival at 10-year follow-up as compared to patients with $\varepsilon_R > 30\%$; (2) $\varepsilon_R$ was independently associated with all-cause mortality.

### 4.1. Cardiac Involvement in SSc Patients

Cardiac involvement in SSc is a challenging diagnosis that, however is an important determinant of adverse prognosis [1,20]. In particular, myocardial dysfunction in these patients is caused by inflammation, ischemia, and fibrosis but it cannot be easily detected [21].

Therefore, even though most patients with SSc initially present without cardiac symptoms, occult primary cardiac involvement may be present and responsible for a significant death rate, reaching 70% at 5 years. As such, careful and timely identification of cardiac involvement is crucial and should include most advanced diagnostic techniques [22–25].

Systolic dysfunction can be diagnosed early in the course of the disease with more sensitive echocardiographic parameters, such as LV GLS. Van Wijngaarden et al. showed in 234 SSc cases, followed-up for a median period of 2.3 years (IQR 1.3–3.9), that LV GLS reduction occurs in a relative short timeframe from diagnosis, even though LVEF did not change over time [26]. In their study, a significant reduction in GLS (i.e., $\geq$15%) was found in 19% of cases, and these patients were more likely to have proximal muscle weakness, lung fibrosis, renal impairment and elevated NTproBNP at follow-up, alongside a higher risk of all-cause mortality [26].

However, in SSc patients, LV diastolic dysfunction is four to five times more frequent as compared to systolic dysfunction. Its assessment is based on a multi-parametric algorithm, in which LAVi plays a central role [3,27]. However, LAVi has limited diagnostic value in the early stages of diastolic dysfunction, while changes in left atrial function have been shown to precede LA dilatation and remodeling and to better correlate with LV filling pressures [4,5,28,29]. Therefore, in the latest EACVI consensus document on imaging in heart failure with preserved ejection fraction, $\varepsilon_R$ is recommended as an additional parameter for the evaluation of LV filling pressures [6].

LA strain and its association with outcome have been evaluated in different studies including different cardiovascular disorders, such as ischemic and valvular heart disease, diabetes, hypertension, and atrial fibrillation [19,30–33]. Furthermore, $\varepsilon_R$ showed a negative association with age [34], and atrial fibrosis quantified by late gadolinium enhancement in CMR studies [35,36].

In SSc, Agoston et al. compared 42 cases with 42 age- and gender-matched controls [7]. The two groups did not differ in respect to LV systolic function or LAVi, but patients with SSc had lower values of $\varepsilon_R$ and higher E/e' [7]. As such, authors concluded that changes in LA strain are able to mirror myocardial fibrosis before abnormalities in LAVi occur, and suggested to use alterations in LA function as an early indicator of cardiac disease in SSc [7].

Another study comparing 72 SSc cases with 30 healthy controls found two thirds of the SSc patients with LV diastolic dysfunction and with reduced $\varepsilon_R$ across all SSc subgroups, further emphasizing that the alteration of LA mechanics might represent an early indicator of cardiac disease in SSc [8]. However, no outcomes were reported by these initial studies.

Recently, a multicentric retrospective study that used feature-tracking CMR-derived strain evaluation of the LV and LA analyzed 100 SSc patients for two endpoints: NYHA class II–IV heart failure symptoms at the time of CMR and all-cause mortality at follow-up [37]. Based on spline curve analysis, a cut-off of 27% for $\varepsilon_R$ was proposed, which was very close to the one identified in the current study [37]. After dichotomizing patients in NYHA I class (39%) and NYHA II-IV class (61%) they observed that $\varepsilon_R$ was associated with the presence of heart failure symptoms at baseline and with all-cause mortality at follow-up [37]. In addition, $\varepsilon_R$ demonstrated incremental prognostic value over the variables known to alter the prognosis of SSc patients [37]. Although this study demonstrated for the first time that lower values of LA strain are associated with higher rates of mortality at follow-up, it was performed using CMR, an advanced imaging method that is not readily available and cannot be repeated easily at follow-up. To the best of our knowledge, our study is the first to assess the correlation between $\varepsilon_R$ measured by echocardiography and all-cause mortality in a large SSc population. By demonstrating its independent association with mortality, it therefore suggests that this parameter might be used to (timely) identify

cardiac involvement and, as such, patients at high risk that might merit closer follow-up or specific treatments.

### *4.2. Limitations*

A few limitations of the current study should be mentioned. The analyzed population included SSc patients referred for screening and extensive evaluation within a specific healthcare program conducted in tertiary care centers, which could have included selection bias (also in terms of disease characteristics). The measurement of LA strain was performed using one vendor and the cut-off values proposed might be not applicable to other echocardiographic vendors. Treatment strategies and their potential association with the outcome were not considered during follow-up; however, considering the absence of homogeneous recommendations, therapeutic changes were also not included in previously published prognostic models. Overall, the findings of the current study should be confirmed in larger, prospective, multicentric studies.

### 5. Conclusions

In SSc patients, left atrial strain $\varepsilon_R \leq 30\%$ is independently associated with all-cause mortality, and as such might be useful in the risk stratification of these patients.

## References

1. Giuca, A.; Gegenava, T.; Mihai, C.M.; Jurcut, C.; Saftoiu, A.; Girnita, D.M.; Popescu, B.A.; Ajmone Marsan, N.; Jurcut, R. Sclerodermic Cardiomyopathy-A State-of-the-Art Review. *Diagnostics* **2022**, *12*, 669. [CrossRef] [PubMed]
2. Tennoe, A.H.; Murbraech, K.; Andreassen, J.C.; Fretheim, H.; Garen, T.; Gude, E.; Andreassen, A.; Aakhus, S.; Molberg, O.; Hoffmann-Vold, A.M. Left Ventricular Diastolic Dysfunction Predicts Mortality in Patients With Systemic Sclerosis. *J. Am. Coll. Cardiol.* **2018**, *72*, 1804–1813. [CrossRef] [PubMed]

3. Nagueh, S.F.; Smiseth, O.A.; Appleton, C.P.; Byrd, B.F., 3rd; Dokainish, H.; Edvardsen, T.; Flachskampf, F.A.; Gillebert, T.C.; Klein, A.L.; Lancellotti, P.; et al. Recommendations for the Evaluation of Left Ventricular Diastolic Function by Echocardiography: An Update from the American Society of Echocardiography and the European Association of Cardiovascular Imaging. *J. Am. Soc. Echocardiogr.* **2016**, *29*, 277–314. [CrossRef] [PubMed]

4. Smiseth, O.A.; Baron, T.; Marino, P.N.; Marwick, T.H.; Flachskampf, F.A. Imaging of the left atrium: Pathophysiology insights and clinical utility. *Eur. Heart J. Cardiovasc. Imaging* **2021**, *23*, 2–13. [CrossRef]

5. Inoue, K.; Khan, F.H.; Remme, E.W.; Ohte, N.; Garcia-Izquierdo, E.; Chetrit, M.; Monivas-Palomero, V.; Mingo-Santos, S.; Andersen, O.S.; Gude, E.; et al. Determinants of left atrial reservoir and pump strain and use of atrial strain for evaluation of left ventricular filling pressure. *Eur. Heart J. Cardiovasc. Imaging* **2021**, *23*, 61–70. [CrossRef]

6. Smiseth, O.A.; Morris, D.A.; Cardim, N.; Cikes, M.; Delgado, V.; Donal, E.; Flachskampf, F.A.; Galderisi, M.; Gerber, B.L.; Gimelli, A.; et al. Multimodality imaging in patients with heart failure and preserved ejection fraction: An expert consensus document of the European Association of Cardiovascular Imaging. *Eur. Heart J. Cardiovasc. Imaging* **2022**, *23*, e34–e61. [CrossRef]

7. Gergely Agoston, L.G.; Miglioranza, M.H.; Caputo, M.; Badano, L.P.; Moreo, A.; Muraru, D.; Mondillo, S.; Pignone, A.M.; Cerinic, M.M.; Sicari, R.; et al. Left atrial dysfunction detected by speckle tracking in patients with systemic sclerosis. *Cardiovasc. Ultrasound* **2014**, *12*, 30. [CrossRef]

8. Porpaczy, A.; Nogradi, A.; Kehl, D.; Strenner, M.; Minier, T.; Czirjak, L.; Komocsi, A.; Faludi, R. Impairment of Left Atrial Mechanics Is an Early Sign of Myocardial Involvement in Systemic Sclerosis. *J. Card. Fail.* **2018**, *24*, 234–242. [CrossRef] [PubMed]

9. Atas, H.; Kepez, A.; Tigen, K.; Samadov, F.; Ozen, G.; Cincin, A.; Sunbul, M.; Bozbay, M.; Direskeneli, H.; Basaran, Y. Evaluation of left atrial volume and function in systemic sclerosis patients using speckle tracking and real-time three-dimensional echocardiography. *Anatol. J. Cardiol.* **2016**, *16*, 316–322. [CrossRef]

10. Meijs, J.; Schouffoer, A.A.; Ajmone Marsan, N.; Kroft, L.J.; Stijnen, T.; Ninaber, M.K.; Huizinga, T.W.; Vliet Vlieland, T.P.; de Vries-Bouwstra, J.K. Therapeutic and diagnostic outcomes of a standardised, comprehensive care pathway for patients with systemic sclerosis. *RMD Open* **2016**, *2*, e000159. [CrossRef]

11. LeRoy, E.C.; Medsger, T.A., Jr. Criteria for the classification of early systemic sclerosis. *J. Rheumatol.* **2001**, *28*, 1573–1576. [PubMed]

12. Yiu, K.H.; Ninaber, M.K.; Kroft, L.J.; Schouffoer, A.A.; Stolk, J.; Scherer, H.U.; Meijs, J.; de Vries-Bouwstra, J.; Tse, H.F.; Delgado, V.; et al. Impact of pulmonary fibrosis and elevated pulmonary pressures on right ventricular function in patients with systemic sclerosis. *Rheumatology* **2015**, *55*, 504–512. [CrossRef]

13. Hansell, D.M.; Bankier, A.A.; MacMahon, H.; McLoud, T.C.; Müller, N.L.; Remy, J. Fleischner Society: Glossary of Terms for Thoracic Imaging. *Radiology* **2008**, *246*, 697–722. [CrossRef]

14. Lang, R.M.; Badano, L.P.; Mor-Avi, V.; Afilalo, J.; Armstrong, A.; Ernande, L.; Flachskampf, F.A.; Foster, E.; Goldstein, S.A.; Kuznetsova, T.; et al. Recommendations for cardiac chamber quantification by echocardiography in adults: An update from the American Society of Echocardiography and the European Association of Cardiovascular Imaging. *Eur. Heart J. Cardiovasc. Imaging* **2015**, *16*, 233–270. [CrossRef] [PubMed]

15. Rudski, L.G.; Lai, W.W.; Afilalo, J.; Hua, L.; Handschumacher, M.D.; Chandrasekaran, K.; Solomon, S.D.; Louie, E.K.; Schiller, N.B. Guidelines for the echocardiographic assessment of the right heart in adults: A report from the American Society of Echocardiography endorsed by the European Association of Echocardiography, a registered branch of the European Society of Cardiology, and the Canadian Society of Echocardiography. *J. Am. Soc. Echocardiogr.* **2010**, *23*, 685–713, quiz 786–688. [CrossRef] [PubMed]

16. Badano, L.P.; Kolias, T.J.; Muraru, D.; Abraham, T.P.; Aurigemma, G.; Edvardsen, T.; D'Hooge, J.; Donal, E.; Fraser, A.G.; Marwick, T.; et al. Standardization of left atrial, right ventricular, and right atrial deformation imaging using two-dimensional speckle tracking echocardiography: A consensus document of the EACVI/ASE/Industry Task Force to standardize deformation imaging. *Eur. Heart J. Cardiovasc. Imaging* **2018**, *19*, 591–600. [CrossRef]

17. Inaba, Y.; Yuda, S.; Kobayashi, N.; Hashimoto, A.; Uno, K.; Nakata, T.; Tsuchihashi, K.; Miura, T.; Ura, N.; Shimamoto, K. Strain rate imaging for noninvasive functional quantification of the left atrium: Comparative studies in controls and patients with atrial fibrillation. *J. Am. Soc. Echocardiogr.* **2005**, *18*, 729–736. [CrossRef]

18. Thomas, L.; McKay, T.; Byth, K.; Marwick, T.H. Abnormalities of left atrial function after cardioversion: An atrial strain rate study. *Heart* **2007**, *93*, 89–95. [CrossRef]

19. Cameli, M.; Lisi, M.; Reccia, R.; Bennati, E.; Malandrino, A.; Solari, M.; Bigio, E.; Biagioli, B.; Righini, F.M.; Maccherini, M.; et al. Pre-operative left atrial strain predicts post-operative atrial fibrillation in patients undergoing aortic valve replacement for aortic stenosis. *Int. J. Cardiovasc. Imaging* **2014**, *30*, 279–286. [CrossRef]

20. Allanore, Y.; Simms, R.; Distler, O.; Trojanowska, M.; Pope, J.; Denton, C.P.; Varga, J. Systemic sclerosis. *Nat. Rev. Dis. Primers* **2015**, *1*, 15002. [CrossRef]

21. Mavrogeni, S.I.; Bratis, K.; Karabela, G.; Spiliotis, G.; Wijk, K.; Hautemann, D.; Reiber, J.H.; Koutsogeorgopoulou, L.; Markousis-Mavrogenis, G.; Kolovou, G.; et al. Cardiovascular Magnetic Resonance Imaging Clarifies Cardiac Pathophysiology in Early, Asymptomatic Diffuse Systemic Sclerosis. *Inflamm. Allergy—Drug Targets* **2015**, *14*, 29–36. [CrossRef] [PubMed]

22. Pokeerbux, M.R.; Giovannelli, J.; Dauchet, L.; Mouthon, L.; Agard, C.; Lega, J.C.; Allanore, Y.; Jego, P.; Bienvenu, B.; Berthier, S.; et al. Survival and prognosis factors in systemic sclerosis: Data of a French multicenter cohort, systematic review, and meta-analysis of the literature. *Arthritis Res. Ther.* **2019**, *21*, 86. [CrossRef] [PubMed]

23. Mani, P.; Gonzalez, D.; Chatterjee, S.; Faulx, M.D. Cardiovascular complications of systemic sclerosis: What to look for. *Cleve Clin. J. Med.* **2019**, *86*, 685–695. [CrossRef]

24. Boueiz, A.; Mathai, S.C.; Hummers, L.K.; Hassoun, P.M. Cardiac complications of systemic sclerosis: Recent progress in diagnosis. *Curr. Opin. Rheumatol.* **2010**, *22*, 696–703. [CrossRef]

25. Hung, G.; Mercurio, V.; Hsu, S.; Mathai, S.C.; Shah, A.A.; Mukherjee, M. Progress in Understanding, Diagnosing, and Managing Cardiac Complications of Systemic Sclerosis. *Curr. Rheumatol. Rep.* **2019**, *21*, 68. [CrossRef] [PubMed]

26. van Wijngaarden, S.E.; Ben Said-Bouyeri, S.; Ninaber, M.K.; Huizinga, T.W.J.; Schalij, M.J.; Bax, J.J.; Delgado, V.; de Vries-Bouwstra, J.K.; Marsan, N.A. Progression of Left Ventricular Myocardial Dysfunction in Systemic Sclerosis: A Speckle-tracking Strain Echocardiography Study. *J. Rheumatol.* **2019**, *46*, 405–415. [CrossRef]

27. Monique Hinchcliff, C.S.D.; Varga, J.; Shah, S.J. Prevalence, Prognosis, and Factors Associated with Left Ventricular Diastolic Dysfunction in Systemic Sclerosis. *Clin. Exp. Rheumatol.* **2012**, *30*, 30–37.

28. Boyd, A.C.; Richards, D.A.; Marwick, T.; Thomas, L. Atrial strain rate is a sensitive measure of alterations in atrial phasic function in healthy ageing. *Heart* **2011**, *97*, 1513–1519. [CrossRef]

29. Morris, D.A.; Belyavskiy, E.; Aravind-Kumar, R.; Kropf, M.; Frydas, A.; Braunauer, K.; Marquez, E.; Krisper, M.; Lindhorst, R.; Osmanoglou, E.; et al. Potential Usefulness and Clinical Relevance of Adding Left Atrial Strain to Left Atrial Volume Index in the Detection of Left Ventricular Diastolic Dysfunction. *JACC Cardiovasc. Imaging* **2018**, *11*, 1405–1415. [CrossRef]

30. Liu, Y.; Wang, K.; Su, D.; Cong, T.; Cheng, Y.; Zhang, Y.; Wu, J.; Sun, Y.; Shang, Z.; Liu, J.; et al. Noninvasive Assessment of Left Atrial Phasic Function in Patients with Hypertension and Diabetes Using Two-Dimensional Speckle Tracking and Volumetric Parameters. *Echocardiography* **2014**, *31*, 727–735. [CrossRef]

31. Mondillo, S.; Cameli, M.; Caputo, M.L.; Lisi, M.; Palmerini, E.; Padeletti, M.; Ballo, P. Early detection of left atrial strain abnormalities by speckle-tracking in hypertensive and diabetic patients with normal left atrial size. *J. Am. Soc. Echocardiogr.* **2011**, *24*, 898–908. [CrossRef] [PubMed]

32. Antoni, M.L.; Ten Brinke, E.A.; Marsan, N.A.; Atary, J.Z.; Holman, E.R.; van der Wall, E.E.; Schalij, M.J.; Bax, J.J.; Delgado, V. Comprehensive assessment of changes in left atrial volumes and function after ST-segment elevation acute myocardial infarction: Role of two-dimensional speckle-tracking strain imaging. *J. Am. Soc. Echocardiogr.* **2011**, *24*, 1126–1133. [CrossRef] [PubMed]

33. Mochizuki, A.; Yuda, S.; Oi, Y.; Kawamukai, M.; Nishida, J.; Kouzu, H.; Muranaka, A.; Kokubu, N.; Shimoshige, S.; Hashimoto, A.; et al. Assessment of left atrial deformation and synchrony by three-dimensional speckle-tracking echocardiography: Comparative studies in healthy subjects and patients with atrial fibrillation. *J. Am. Soc. Echocardiogr.* **2013**, *26*, 165–174. [CrossRef]

34. Pathan, F.; D'Elia, N.; Nolan, M.T.; Marwick, T.H.; Negishi, K. Normal Ranges of Left Atrial Strain by Speckle-Tracking Echocardiography: A Systematic Review and Meta-Analysis. *J. Am. Soc. Echocardiogr.* **2017**, *30*, 59–70.e58. [CrossRef] [PubMed]

35. Marrouche, N.F.; Wilber, D.; Hindricks, G.; Jais, P.; Akoum, N.; Marchlinski, F.; Kholmovski, E.; Burgon, N.; Hu, N.; Mont, L.; et al. Association of Atrial Tissue Fibrosis Identified by Delayed Enhancement MRI and Atrial Fibrillation Catheter Ablation: The DECAAF Study. *JAMA* **2014**, *311*, 498–506. [CrossRef]

36. Kuppahally, S.S.; Akoum, N.; Burgon, N.S.; Badger, T.J.; Kholmovski, E.G.; Vijayakumar, S.; Rao, S.N.; Blauer, J.; Fish, E.N.; Dibella, E.V.; et al. Left atrial strain and strain rate in patients with paroxysmal and persistent atrial fibrillation: Relationship to left atrial structural remodeling detected by delayed-enhancement MRI. *Circ. Cardiovasc. Imaging* **2010**, *3*, 231–239. [CrossRef]

37. Butcher, S.C.; Vos, J.L.; Fortuni, F.; Galloo, X.; Liem, S.I.E.; Bax, J.J.; Delgado, V.; Vonk, M.C.; van Leuven, S.I.; Snoeren, M.; et al. Evaluation of Left Cardiac Chamber Function with Cardiac Magnetic Resonance and Association with Outcome in Patients with Systemic Sclerosis. *Rheumatology* **2023**, *62*, SI20–SI31. [CrossRef]